Application of Collocation Meshless Method to Eigenvalue Problem*)

Ayumu SAITOH, Taku ITOH[1)], Nobuyuki MATSUI, Atsushi KAMITANI[2)] and Hiroaki NAKAMURA[3)]

University of Hyogo, Himeji, Hyogo 671-2280, Japan
[1)]*Seikei University, Musashino, Tokyo 180-8633, Japan*
[2)]*Yamagata University, Yonezawa, Yamagata 992-8510, Japan*
[3)]*National Institute for Fusion Science, Toki, Gifu 509-5292, Japan*

(Received 9 December 2011 / Accepted 18 May 2012)

The numerical method for solving the nonlinear eigenvalue problem has been developed by using the collocation Element-Free Galerkin Method (EFGM) and its performance has been numerically investigated. The results of computations show that the approximate solution of the nonlinear eigenvalue problem can be obtained stably by using the developed method. Therefore, it can be concluded that the developed method is useful for solving the nonlinear eigenvalue problem.

Keywords: element-free Galerkin method, finite element method, nonlinear eigenvalue problem, Grad-Shafranov equation, numerical analysis

DOI: 10.1585/pfr.7.2406096

1. Introduction

As is well known, the Grad-Shafranov (G-S) equation describes the magnetohydrodynamics equilibrium of plasma in terms of the poloidal magnetic flux ψ. Once a set of parameters is given, this equation and its associated boundary conditions constitute a nonlinear boundary-value problem with an eigenvalue λ. Many numerical methods have been so far proposed and have yielded excellent results in the fields of plasma physics and nuclear fusion [1,2].

On the other hand, many meshless methods [3,4] have been proposed and have been used in the fields of engineering and science. In spite of the convenience, meshless methods are plagued by two difficulties. First, the method for implementing the essential boundary condition is different according to meshless methods. Second, both the essential boundary condition and the natural one are not exactly fulfilled on the boundary. If a new implementation method of not only the essential boundary condition but also the natural one were proposed without dependence on meshless methods, the above demerit could be completely resolved.

In the previous studies, Kamitani *et al*. [5] have proposed the new method for implementing the essential boundary condition to the meshless Galerkin/Petrov-Galerkin approach. The results of computations have shown that the accuracy of the Kamitani's meshless method is higher than that of the standard one. In addition, Saitoh *et al*. [6] have extended the above method and have applied it to the nonlinear Poisson problem.

The purpose of the present study is to develop the numerical method for solving the nonlinear eigenvalue problem by using the collocation Element-Free Galerkin Method (EFGM) [5] and to numerically investigate its performance.

2. Numerical Method of Nonlinear Eigenvalue Problem

2.1 Linearization

For simplicity, we consider the following nonlinear eigenvalue problem in axisymmetric coordinate system (r, z):

$$-\hat{L}\psi = \rho(\lambda, r, \psi) \qquad \text{in } \Omega, \tag{1}$$

$$\psi = 0 \qquad \text{on } \partial\Omega. \tag{2}$$

Here, Ω denotes a domain bounded by a simple closed curve $\partial\Omega$, and $\rho(\lambda, r, \psi)$ is a known function in Ω. Furthermore, $\hat{L}$ denotes the G-S operator defined by

$$\hat{L} \equiv \frac{\partial^2}{\partial z^2} + r\frac{\partial}{\partial r}\left(\frac{1}{r}\frac{\partial}{\partial r}\right).$$

Since (1) has a nonlinearity, the above problem is difficult to solve analytically. In this study, an approximate solution is calculated in such a way that the total plasma current is always preserved through the iteration. In the kth step, we solve the following linear problem for $\psi^{(k+1)}$:

$$-\hat{L}\psi^{(k+1)} = \rho(\lambda^{(k)}, r, \psi^{(k)}) \qquad \text{in } \Omega, \tag{3}$$

$$\psi^{(k+1)} = 0 \qquad \text{on } \partial\Omega, \tag{4}$$

author's e-mail: saitoh@eng.u-hyogo.ac.jp

*) This article is based on the presentation at the 21st International Toki Conference (ITC21).

where the superscript (k) is an iteration number label. Subsequently, the eigenvalue $\lambda^{(k+1)}$ is calculated by use of the relation:

$$I_p = \iint_\Omega \frac{1}{r}\rho(\lambda^{(k+1)}, r, \psi^{(k+1)})\,\mathrm{d}z\mathrm{d}r, \tag{5}$$

where I_p is a constant. Finally, the approximate solution and the approximate eigenvalue are updated by use of the underrelaxation ω: $\psi^{(k+1)} = \psi^{(k)} + \omega\left[\psi^{(k+1)} - \psi^{(k)}\right]$ and $\lambda^{(k+1)} = \lambda^{(k)} + \omega\left[\lambda^{(k+1)} - \lambda^{(k)}\right]$. The above step is repeated until both $|\lambda^{(k+1)} - \lambda^{(k)}|/|\lambda^{(k+1)}| \le 10^{-6}$ and $\|\psi^{(k+1)} - \psi^{(k)}\|/\|\psi^{(k+1)}\| \le 10^{-6}$ are satisfied. Here, the maximum norm is adopted for the definition of $\|\ \|$. Throughout the present study, the above iteration is called an outer iteration. In this way, the nonlinear eigenvalue problem (1)-(2) is reduced to the problem in which (3) and (4) are solved by use of the iterative method.

As is well known, (3) is satisfied if and only if the following weak form is fulfilled:

$$\forall w \text{ s.t. } w\big|_{\partial\Omega} = 0 : \iint_\Omega \frac{1}{r}\nabla w \cdot \nabla\psi^{(k+1)}\,\mathrm{d}z\mathrm{d}r - \iint_\Omega w\frac{\rho(\lambda^{(k)}, r, \psi^{(k)})}{r}\,\mathrm{d}z\mathrm{d}r = 0, \tag{6}$$

where $\forall w \text{ s.t. } w\big|_{\partial\Omega} = 0$ denotes an arbitrary function $w(\boldsymbol{x})$ that satisfies $w = 0$ on $\partial\Omega$.

As mentioned in the section 1, the method for implementing the essential boundary condition is different according to meshless methods. For example, as the implementation method, the Lagrange multiplier and the penalty method are used in the standard EFGM [3] and the meshless local Petrov-Galerkin method [4], respectively. In the present study, the collocation EFGM, in which the above demerit is resolved, is adopted as the discretization of (6).

2.2 Discretization

In order to discretize (6), let us first place nodes, $\boldsymbol{x}_1, \boldsymbol{x}_2, \cdots, \boldsymbol{x}_N$, in $\Omega \cup \partial\Omega$. Next, shape functions ϕ_i's are determined by using the Moving Least-Squares (MLS) approximation [3]. Finally, both the trial function $\psi^{(k+1)}(\boldsymbol{x})$ and the test function $w(\boldsymbol{x})$ are assumed to be contained in the functional space $V \equiv \mathrm{span}\,(\phi_1, \phi_2, \cdots, \phi_N)$, i.e., $\psi^{(k+1)}(\boldsymbol{x})$ and $w(\boldsymbol{x})$ are assumed as

$$\psi^{(k+1)}(\boldsymbol{x}) = \sum_{i=1}^{N}\phi_i(\boldsymbol{x})\,\hat{\psi}_i^{(k+1)},$$

$$w(\boldsymbol{x}) = \sum_{i=1}^{N}\phi_i(\boldsymbol{x})\,\hat{w}_i,$$

where $\hat{\psi}_i^{(k+1)}$ and $\hat{w}_i$ $(i = 1, 2, \cdots, N)$ are all constants. In the following, M denote the number of nodes on $\partial\Omega$. In addition, $\{\boldsymbol{e}_1, \boldsymbol{e}_2, \cdots, \boldsymbol{e}_N\}$ and $\{\boldsymbol{e}_1^*, \boldsymbol{e}_2^*, \cdots, \boldsymbol{e}_M^*\}$ are the orthogonal system of the N-dimensional vector space and that of M-dimensional vector space, respectively.

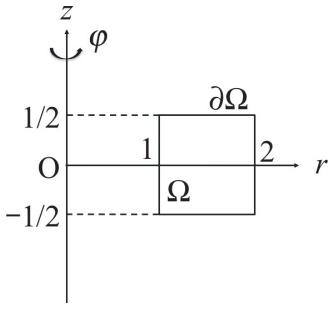

Fig. 1 Domain Ω and its boundary $\partial\Omega$.

From the standard manner of the collocation EFGM, the weak form (6) and its associated boundary condition (2) are discretized. The resulting equations can be written in the following form:

$$\begin{bmatrix} A & C \\ C^T & \mathrm{O} \end{bmatrix}\begin{bmatrix} \hat{\boldsymbol{\psi}}^{(k+1)} \\ \hat{\boldsymbol{\nu}}^{(k+1)} \end{bmatrix} = \begin{bmatrix} \boldsymbol{f}^{(k)} \\ \boldsymbol{0} \end{bmatrix}. \tag{7}$$

Here, $\hat{\boldsymbol{\psi}}^{(k+1)}$ and $\hat{\boldsymbol{\nu}}^{(k+1)}$ are defined by

$$\hat{\boldsymbol{\psi}}^{(k+1)} = \sum_{i=1}^{N}\hat{\psi}_i^{(k+1)}\boldsymbol{e}_i, \qquad \hat{\boldsymbol{\nu}}^{(k+1)} = \sum_{i=1}^{M}\hat{\nu}_i^{(k+1)}\boldsymbol{e}_i^*,$$

where $\hat{\nu}_i^{(k+1)}$ $(i = 1, 2, \cdots, M)$ are all constants. In addition, A, C and $\boldsymbol{f}^{(k)}$ are given by

$$A = \sum_{i=1}^{N}\sum_{j=1}^{N}\iint_\Omega \frac{1}{r}\nabla\phi_i \cdot \nabla\phi_j\,\mathrm{d}z\mathrm{d}r\,\boldsymbol{e}_i\boldsymbol{e}_j^T,$$

$$C = \sum_{i=1}^{N}\sum_{p=1}^{M}\phi_i(\boldsymbol{x}(s_p))\,\boldsymbol{e}_i\boldsymbol{e}_p^{*T},$$

$$\boldsymbol{f}^{(k)} = \sum_{i=1}^{N}\iint_\Omega \phi_i\frac{\rho(\lambda^{(k)}, r, \psi^{(k)})}{r}\,\mathrm{d}z\mathrm{d}r\,\boldsymbol{e}_i,$$

where s_p denotes an length along the boundary from $\boldsymbol{x}_1$ to $\boldsymbol{x}_p$.

By solving (7) iteratively, we can get the approximate solution of the nonlinear eigenvalue problem. Note that the coefficient matrix in (7) becomes symmetiry and sparse. In this study, we adopt the Incomplete Cholesky Conjugate Gradient (ICCG) method as the solver of (7) [7].

3. Numerical Results

The numerical method for solving the nonlinear eigenvalue problem has been developed on the basis of the collocation EFGM. In this section, we numerically investigate its performance.

Throughout the present study, the domain Ω is given by $\Omega = (1, 2) \times (-1/2, 1/2)$ (see Fig. 1). Moreover, the nodes are uniformly placed in $\Omega \cup \partial\Omega$. In the MLS approximation, a linear basis $\boldsymbol{p}^T(\boldsymbol{x}) = [1, x, y]$ and the Gaussian-type weight function are assumed. The explicit form of the weight function is given by

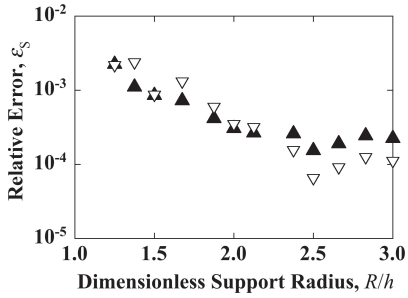

Fig. 2 Dependence of the relative error ϵ_S on the dimensionless support radius R/h. Here, ▲ : $N = 411$ and ▽ : $N = 969$.

$$w_i(\boldsymbol{x}) = w\left(|\boldsymbol{x} - \boldsymbol{x}_i|\right),$$

$$w(\tilde{r}) = \begin{cases} \frac{\exp\left[-(\tilde{r}/c)^2\right] - \exp\left[-(R/c)^2\right]}{1 - \exp\left[-(R/c)^2\right]} & ;\tilde{r} \le R, \\ 0 & ;\tilde{r} > R, \end{cases}$$

where R denotes a support radius and c is a constant. In this study, the value of c is equal to the minimum distance h between two nodes.

3.1 Performance evaluation of developed method

In the section 3.1, we compare the performance of the developed method with the method based on the Finite Element Method (FEM) by solving the boudnary-value problem of the linear G-S equation. In the present section, ρ is assumed as $\rho = -\left[(\pi(1-4z^2))\cos\pi r + (8 + \pi^2(1-4z^2))r\sin\pi r\right]/4r$, i.e., the analytic solution of the G-S problem is given by

$$\psi = \left(\frac{1}{4} - z^2\right)\sin\left[\pi\left(r-1\right)\right].$$

Let us first investigate the influence of the support radius on the accuracy of the numerical solution. As the measure of the accuracy, we adopt the relative error: $\varepsilon_S \equiv \|\psi_A - \psi_N\|/\|\psi_A\|$ where subscript notations, A and N, indicate analytic and numerical solutions, respectively. The relative error ε_S is calculated as a function of the dimensionless support radius R/h and is depicted in Fig. 2. We see from this figure that the relative error roughly decreases with R/h until it becomes almost constant for $R/h \gtrsim 2.5$. These behaviors do not change qualitatively regardless of the value of N. In the following, the value of R/h is fixed as $R/h = 2.5$.

Next, we compare the accuracy of the developed method with that of the method based on the FEM. In the following experiments, triangular elements are generated by dividing the domain Ω into $N_x \times N_y$ pieces of small rectangles and inserting a diagonal line to each rectangle. Therefore, the number N of nodes and the number M of elements satisfy $N = (N_x + 1) \times (N_y + 1)$ and $M = 2N_xN_y$, respectively. The relative error ε_S is calculated as a function of the number N of nodes and is depicted in Fig. 3. Both relative error of the developed method and that of the method based on the FEM are almost proportional to $N^{-\beta}$.

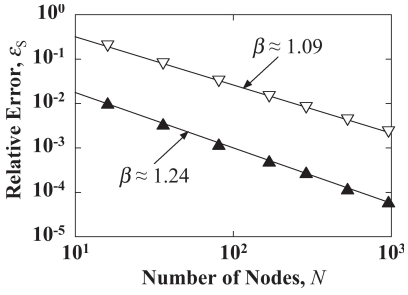

Fig. 3 Dependence of the relative error ϵ_S on the number N of nodes. Here, ▲: the collocation EFGM and ▽ : the FEM.

Power indeces of the developed method and the method based on the FEM satisfy $\beta \approx 1.24$ and $\beta \approx 1.09$, respectively. In other words, the convergence rate of the developed method is higher than that of the method based on the FEM.

From these results, we can conclude that the accuracy of the developed method is higher than that of the method based on the FEM.

3.2 Application to nonlinear eigenvalue problem

In accord with these results of the section 3.1 , we apply the developed method to the nonlinear eigenvalue problem. In the following, $\rho(\lambda, r, \psi)$ is given by

$$\rho(\lambda, r, \psi) = \lambda\psi\left[1 - \gamma\left(\frac{\psi}{\psi_{\max}}\right)\right],$$

where γ is a constant and $\psi_{\max}$ is the maximum value of $\psi(\boldsymbol{x})$. In addition, the initial eigenvalue $\lambda^{(1)}$ and the initial solution $\psi^{(1)}$ are defined by

$$\lambda^{(1)} = 2\pi^2, \tag{8}$$

$$\psi^{(1)} = \sin\left[\pi\left(z - \frac{1}{2}\right)\right]\sin\left[\pi\left(r-1\right)\right]. \tag{9}$$

Let us first investigate the number of the outer iteration for the case with $\gamma = 0$. Hereafter, the number of the outer iteration required for the convergence is called the convergence iteration number. In the inset of Fig. 4, we show the dependence of the convergence iteration number k_C on the number N of nodes. This figure indicates that k_C satisfies $k_C \approx 13$. In other words, the convergence iteration number becomes almost constant regardless of N. As a result, we can get the convergent solution for the case with $N < 10^3$.

Next, we investigate the influence of the number of nodes on the accuracy of the developed method. The analytic eigenvalue can be determined if and only if $\gamma = 0$. Therefore, we adopt the relative error ε_L defined by $\varepsilon_L \equiv |\lambda_A - \lambda_N| / |\lambda_A|$ as the measure of the accuracy. Figure 4 indicates the dependence of the relative error ε_L on the number N of nodes for the case with $\gamma = 0$. We see from this figure that the relative error drastically improves with an increase in N for $N \lesssim 10^2$. After that, it gradually en-

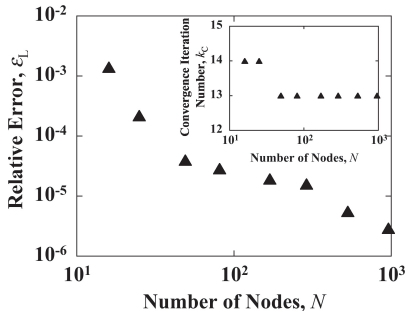

Fig. 4 Dependence of the relative error ϵ_L on the number N of nodes. The inset indicates the dependence of the convergent iteration number k_C on the number N of nodes. In these above figures, the parameters are fixed as follows: $\gamma = 0$ and $\omega = 1$.

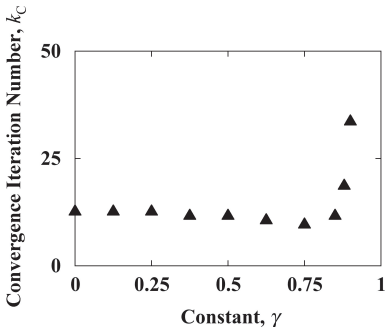

Fig. 5 Dependence of the convergent iteration number k_C on the constant γ for the case with $N = 969$ and $\omega = 1$.

hances with an increase in N.

Finally, we investigate the influence of the constant γ on the number of the outer iteration. The convergence iteration number k_C is calculated as a function of the constant γ and is depicted in Fig. 5. We see from this figure that k_C becomes almost constant until it drastically increases for $0.85 \lesssim \gamma \leq 0.9$. In addition, for the case with $\gamma > 0.9$, the approximate solution cannot be obtained.

Residual norm histories of the eigenvalue and the solution are shown in Figs. 6 (a) and 6 (b), respectively. For the case with $\omega = 1$ and $\omega = 0.85$, both the residual norms of the eigenvalue and the solution do not converge. In contrast, the termination condition is fulfilled for $\omega = 0.75$. Hence, the approximate solution can be obtained by using the appropriate value of ω.

From these results, we can conclude that the developed method is useful as the numerical method of the boudnary-value problem of the nonlinear G-S equation.

4. Conclusion

The numerical method for solving the nonlinear eigenvalue problem has been developed on the basis of the collocation EFGM and its performance has been numerically investigated. The results of computations show that the approximate solution of the nonlinear eigenvalue problem can be obtained stably by using the developed method.

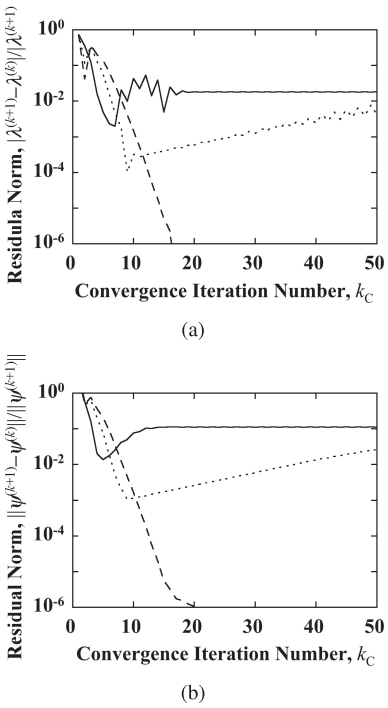

Fig. 6 The residual norm histories of (a) the eigenvalue and (b) the solution for the case with $N = 969$ and $\gamma = 0.95$. Here, $(--)$: $\omega = 0.75$, $(\cdots)$: $\omega = 0.85$ and (—): $\omega = 1$.

Therefore, it can be concluded that the developed method is useful for solving the nonlinear eigenvalue problem.

We have applied the developed method to the nonlinear eigenvalue problem. However, its performance has not been investigated in detail. As the future work, we will compare the simulation result with the experiment one by using a physical parameter. In addition, it will be also necessary to investigate the suitable solver for the nonlinear eigenvalue problem.

Acknowledgement

This work was supported in part by Japan Society for the Promotion of Science under a Grant-in-Aid for Scientific Research (B) No. 22360042. A part of this work was also performed with the support and under the auspices of the NIFS Collaboration Research Program (NIFS11KNTS011, NIFS11KNTS014).

[1] S. Ikuno, A. Kamitani and M. Natori, J. JSAEM **6(1)**, 63 (1998) [in Japanese].
[2] M. Itagaki and T. Fukunaga, Eng. Anal. Boundary Elements **30**, 746 (2006).
[3] T. Belytchko, Y.Y. Lu and L. Gu, Int. J. Numer. Methods Eng. **37**, 229 (1994).
[4] S.N. Atluri and T. Zhu, Comput. Mech. **22(2)**, 117 (1998).
[5] A. Kamitani, T. Takayama, T. Itoh and H. Nakamura, Plasma Fusion Res. **6**, 2401074 (2011).
[6] A. Saitoh, T. Itoh, N. Matsui and A. Kamitani, IEEE Trans. Magn. **48(2)**, 487 (2012).
[7] J. Meijerink and H.A. van der Vorst, Math. Comput. **31**, 148 (1977).